2021 43rd Annual International Conference of the
IEEE Engineering in Medicine & Biology Society (EMBC)
Oct 31 - Nov 4, 2021. Virtual Conference

A Novel Asymmetric Pneumatic Soft-Surgical Endoscope Design with Laminar Jamming

Nehal Mathur[1], Yoeko X. Mak[1], Hamid Naghibi[1] and Momen Abayazid*[1]

***Abstract*— Soft pneumatic endoscopes developed for Minimally Invasive Surgeries (MIS) are designed upright which means that the starting positions straight. As the internal chambers are pressurized the endoscopic module starts bending. The relation between the pneumatic pressure and bending is nonlinear as the air needs first to fill the chamber before bending, and additionally frictional interaction to the sheath adds more to this start-up transient behaviour. This highly nonlinear behaviour severely limits the actuator sensitivity, accuracy, and repeatability near the endoscope's center of operating range. This paper introduces a novel pre-bent MR-compatible soft-surgical pneumatic endoscope design aimed to improve the bending performance of soft endoscopes by shifting the start-up transient out of the operating range. The pre-bent design of 12 mm diameter consists of an actuation and stiffening chamber, inextensible shell reinforcement with a backbone and rings, and external sheathing. The design parameters that include cross-sectional area, number of rings and backbone width are determined using Finite Element (FE) analysis. The motion profile of the fabricated endoscope, determined via experimentation, shows a successful shift of the start-up transient while the jamming structure increases the stiffness of the endoscope but limits the bending range. Further design developments of the endoscope are required for clinical application.**

I. INTRODUCTION

The general trend observed in medicine regarding abdominal surgeries is the increased preference for Minimally Invasive Surgery (MIS). Some advantages of MIS are drastically reducing patient recovery time, reduced pain and lower blood loss [1], [2]. Majority of minimally invasive procedures require the use of endoscopic camera for visual feedback.

There are two types of endoscopes; rigid and flexible. Rigid endoscopes are used for surgical targets close to the incision point since they have limited motion and difficulty maneuvering around healthy organs to reach a difficult surgical target [3]. Their rigidity enables surgeons to exert necessary forces when performing surgical tasks. However, due to the fulcrum effect surgeon's movements are inverted and tremors amplified giving rise to instability [4].

On the other hand, flexible endoscopes have the required manoeuvrability but lack the adjustable stiffness necessary to perform the surgery [5]. Another issue with flexible endoscopes is localization since it is difficult to track internally, as the camera's lack of depth perception and horizon stability provides insufficient information to determine the position of the distal tip or the rest of the insertion tube [6], [7].

Soft endoscopes are a rapidly growing research field. Inspired by nature, it uses flexible and compliant materials in the design and actuation of robotic systems [8], [9]. This compliant feature is ideal for an endoscope that is required to bend, deform and be inserted deep without damaging its surroundings [10]. An intrinsic benefit of soft-robotics is its inherent MRI-compatibility since it is pneumatically actuated, which enables the localisation of the endoscope during the procedure [11].

Pneumatic bending actuators rely on the pressurisation of chambers resulting in the desired actuation but also radial expansion. Several state of the art soft pneumatic endoscopes are developed upright encased in sheathing to prevent radial expansion [12], [13], [14], [15]. This affects the performance of the endoscope as it induces start-up behaviour, such as the dead-zone and low sensitivity region shown in Figure 1. The dead-zone is a result of the margin between the elastomer and the inner diameter of the external sheathing, and its frictional interaction when the chamber is pressurized. This highly nonlinear behaviour severely limits the actuator sensitivity, accuracy, and repeatability near the endoscope's straight configuration.

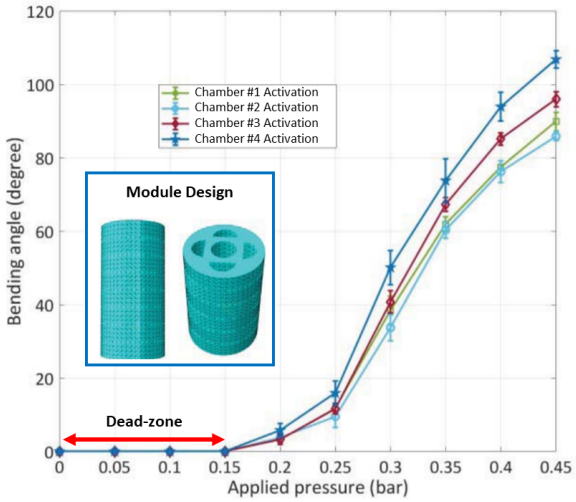

Fig. 1: Motion profile of a pneumatic soft endoscope designed with four actuation chambers consisting of a dead-zone in the upright position. [16]

Therefore, in this paper we present a novel miniaturised flexible soft-surgical endoscope design to shift the start-up

*This work was supported in part by ITEA3 under 17021 IMPACT project.

[1] N. Mathur, Y. X. Mak, H. Naghibi and M. Abayazid are with the Robotics and Mechatronics Laboratory, Technical Medical Centre at University of Twente, 7522 NH Enschede, the Netherlands. Email: nehalmathur@gmail.com, y.x.mak@utwente.nl, h.naghibibeidokhti@utwente.nl, m.abayazid@utwente.nl

TABLE I: An overview of several flexible endoscope designs in research and clinical domain.

Technology	Outer Diameter (mm)	Max Bending	MRI-Compatible	Variable stiffness
MINIR [17]	12.6	90°	Yes	No
STIFF-FLOP (V1) [12]	35.0	120°	Yes	Yes
STIFF-FLOP (V2) [14]	25.0	120°	Yes	Yes
STIFF-FLOP (V3) [3]	14.7	120°	Yes	No
MOLLUSC [16]	30.0	100°	Yes	Yes
Invendoscope [18], [19], [20]	18.0	180°	No	No
NeoGuide [18], [19]	20.0-14.0	∼	No	Yes
Olympus ENDOEYE FLEX [21]	10.0/5.0	100°	No	No
Olympus DCE [22]	12.2	140°	No	No

behaviour location, thereby improving motion control of the soft endoscope in the operating range. Several design parameters have been analysed along with the performance of the novel design using Finite Element (FE) modeling. Finally, the bending performance of the fabricated endoscope, based on experimental results, is presented and discussed.

II. DESIGN, ANALYSIS, AND FABRICATION

The main objective of the design is shifting the start-up behaviour out of the operating range of the endoscope. While the previously designed prototype [16] can bend more than 90° on each side, the dead-zone and the nonlinear start-up behaviour are located at the center of its operating range. To shift the start-up transient out of the operating range, the endoscope starts pre-bent. Therefore, unlike conventional flexible endoscope designs, the novel endoscope begins bent when at rest and straightens when actuated.

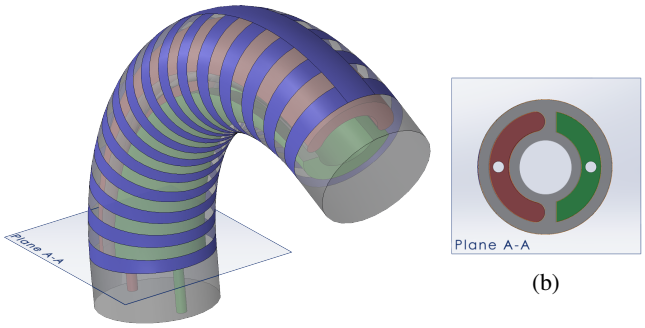

(a) (b)

Fig. 2: Design of the pre-bent endoscope module. The color highlighting indicates various sections of the module: the actuation chamber (green), stiffening chamber (red), and the combined backbone with rings (blue). Image in (b) shows the cross-section of the endoscope's silicone inner module.

A. Design of Pre-Bent Soft Endoscope

The design is based on the single chamber shell-reinforced soft pneumatic actuator and is shown in Figure 2. The endoscope's main body consists of the actuation chamber, stiffening chamber and a free central lumen of 4.5 mm in diameter. It is encased with an in-extensible shell consisting of a backbone and rings. The shell-reinforcement designed is similar to that used in the bending pneumatic actuator, with rings attached to a backbone that runs along the outer arc of the bent actuator. Thus, the rings are further apart along the outer arc and closer together along the inner arc. When the actuator is pressurised, the backbone will inhibit the extension of the module while the rings will limit radial expansion. The shell-reinforcement enables the bending of the endoscope until it becomes straight. A bending angle of 120° at rest is chosen to match the performance and capabilities of endoscopes presented in Table I.

The chosen variable stiffening mechanism is laminar jamming where the number and dimensions of the sheets are determined using an analytical model [23]. It is influenced by the available space and desired force output (between 0.9 and 3.3 N [15]). The maximum stiffness of the jamming structure is defined as:

$$k_{\max} = \frac{8Ew(Nh)^3}{12L^4} \tag{1}$$

Therefore, in combination with the FE results discussed later, stiffness is maximised with the largest possible width (w) and number of sheets (N). The stiffening chamber is located next to the backbone and the actuation chamber is opposite to it. This configuration is chosen to limit the radial expansion (ballooning) by placing the actuation chamber along the inner arc where the rings are placed closer together.

Since there are portions of the endoscope that are not entirely covered by shell reinforcement, an additional sheathing is required to constrain excessive radial expansion. This will strengthen the module by adding stiffness as well as drastically decreasing the chances of mechanical failure at high pressures due to ballooning and rupture.

B. Finite Element Analysis

In order to asses the design aspects of the endoscopic module, an FE model of the concept was developed. The endoscope is modeled within COMSOL Multiphysics Version 5.5 with a combination of solid mechanics (main body), membrane (backbone) and truss (rings) elements. The material properties of modelled parts can be found in Table II, where Neo-Hookean hyper-elastic material model is used for Ecoflex 00-30 (Smooth-on Inc, Pennsylvania, USA). The endoscope modelled consists of only the actuation chamber with the stiffening chamber and the free central lumen modelled as 'filled' to represent the endoscope state when used in clinical applications.

TABLE II: Material properties used for FE analysis in COMSOL.

Material	Young's Modulus (E)	Poisson's Ratio (ν)	Density (kg/m^3)	Part
Ecoflex 00-30	27.04 kPa	0.43	1000	Main body
Acrylic	3.2 GPa	0.35	1190	Shell-reinforcement
Paper-coated-plastic	200G Pa	0.20	940	Jamming structure

The performance of the endoscope and the influence of several design parameters are determined using FE analysis. Geometric properties such as the cross-sectional area, the number of rings and the width of the backbone all effect the performance of the endoscope. The design variations of each are depicted in Figure 4. This is a measure of the amount

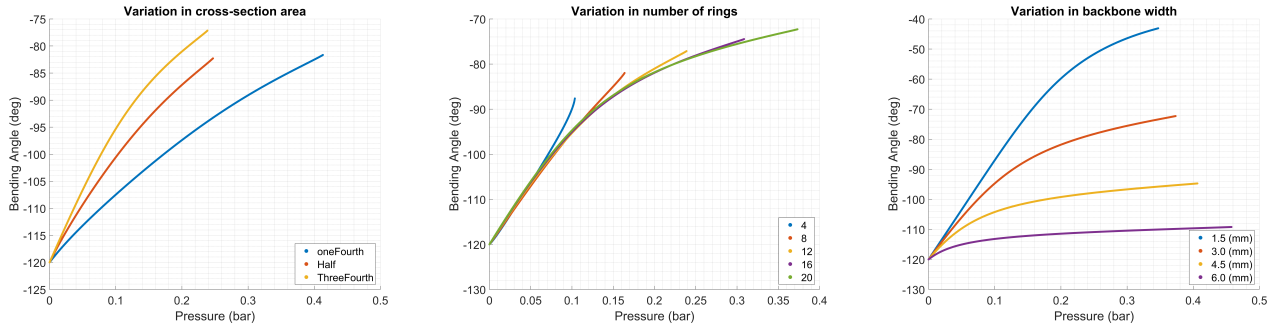

(a) (b) (c)

Fig. 3: Finite Element analysis of novel pre-bent endoscope design with varying design parameters such as (a) the cross-sectional area of the actuation chamber, (b) the number of rings of the shell-reinforcement and (c) the width of the backbone to which the rings are attached.

of bending for an applied pressure. The ideal performance is for the endoscope to bend with as little applied pressure as possible.

1) Cross-Sectional Area: The cross-sectional area of the actuation chamber is varied by $\frac{1}{4}$, $\frac{1}{2}$ and $\frac{3}{4}$ of the circumference of the endoscope. The cross-sectional area is proportional to the bending moment and therefore directly influences the bending performance. Figure 3a shows this expected behaviour, where the design with the largest cross-sectional area has the largest bending to pressure sensitivity. However, a large actuation chamber limits the space available for the implementation of the stiffening mechanism resulting in the cross-sectional area of $\frac{1}{2}$ being chosen.

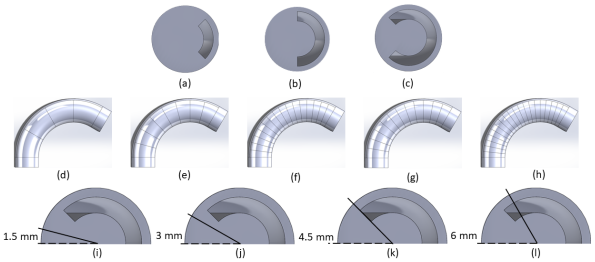

Fig. 4: The geometric variations for the design study. (a - c) depicts the cross-sectional area of the actuation chamber, (d - h) depicts the number of rings and (i - l) depicts the backbone width.

2) Number of Rings: The number of rings are varied from 4 to 20 with increments of 4. Ballooning during actuation decreases with a larger number of rings [24]. The maximum bending angle is expected to improve with a larger number of rings since they limit ballooning. Figure 3b shows that all designs have similar motion profiles initially, deviating only after model stiffness decreases due to the effect of ballooning. Although the bending performance of the design increases, its maximum bending is affected. Ballooning weakens the actuator wall by decreasing its thickness. A maximum of 16 rings were chosen for the design due to fabrication limitations.

3) Backbone Width: The backbone runs along the outer arc of the endoscope and its width is varied between 1.5 to 6.0 mm with increments of 1.5 mm. Since the backbone is modeled as an in-extensible material, a larger backbone width should increase the stiffness of the model and therefore inhibit the bending performance. The result from the FE analysis is presented in Figure 3c. The backbone width of 1.5 mm was employed due to its low contribution to the overall stiffness and largest bending to pressure sensitivity.

The chosen design parameters are implemented into the design and its FE simulation is shown in Figure 5a.

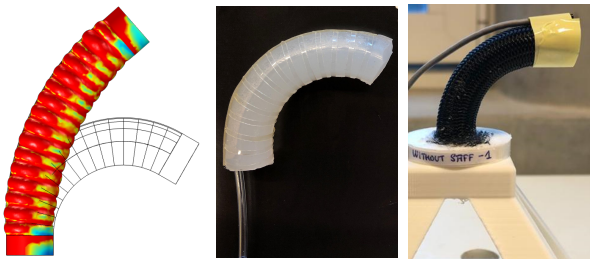

(a) (b) (c)

Fig. 5: The FE simulation of the modelled endoscope in (a) depicting the bending performance, ballooning and functionality of the inextensible backbone and rings. The fabricated endoscope without (b) and with (c) external sheathing.

C. Fabrication

The fabrication process of the endoscope is divided into three stages: elastomer moulding, shell-reinforcing and external sheathing. The elastomer moulding fabricates the main body of the endoscope using Ecoflex 00-30 with the two empty chambers. Laminar jamming sheets are stacked and inserted into the stiffening chamber. The inextensible shell is produced using a thin laser cut plastic sheet which is placed around the elastomer main body, depicted in Figure 5b. Finally, an external sheath is added to restrict any excessive radial expansion as a result of actuation. Disparity in the rest position of the FE simulations and the fabricated

endoscope arise from fabrication errors. This can be seen in the difference in rest position in Figure 5b and Figure 5c.

III. EXPERIMENTAL CHARACTERISATION

The motion characterisation curve maps the relationship between the bending of the endoscope tip to an applied pressure.

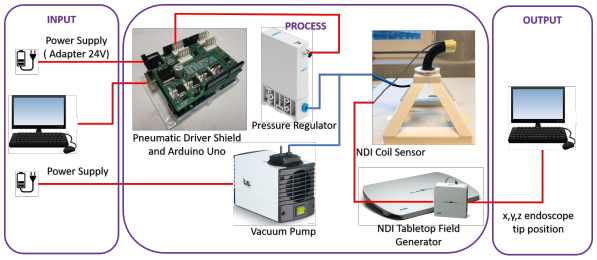

Fig. 6: The experimental setup for the motion characterisation of the completely fabricated endoscope.

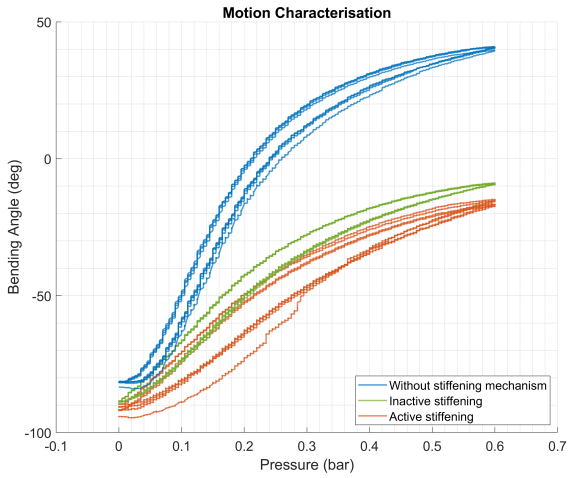

Fig. 7: Bending performance of endoscope without the stiffening mechanism (blue), with inactive stiffening mechanism (green) and activated stiffening mechanism (red). Activation refers to the vacuuming of the stiffening chamber. The data is gathered over four repeated increasing and decreasing actuation cycles for each measurement.

A. Setup

The bending performance of the endoscope when pressurised is measured using the NDI Aurora position sensor (NDI Medical, Ontario, Canada). The endoscope is placed on the Aurora Tabletop Field Generator and the position sensor is attached to the tip of the endoscope along the outer arc, parallel to the backbone, shown in Figure 6. The soft endoscope module is actuated by gradually increasing and then decreasing the pressure from 0 to 0.6 bar. During the procedure, input pressure and tip orientation is measured over four increasing and decreasing actuation cycles.

B. Results and Discussion

The bending performance of the endoscope with and without the activation of the stiffening mechanism is in Figure 7. In both cases the endoscope begins at a pre-bent position of -88° with a maximum bending angle of -10° when stiffening is inactive and -16° when stiffening is active. The start-up transient is significantly lower when stiffening is inactive, lasting for a maximum of 0.01 bar. An active stiffening mechanism induces a larger static friction resulting in a larger dead-zone, present for a maximum input pressure of 0.03 bar. The dead-zone, compared to Figure 1, is minimised due to the addition of rings as they are attached directly to the body of the endoscope and therefore limit the initial radial expansion.

Saturation in the bending performance of the endoscope is present at high pressures due to an increase in stiffness. The rate of saturation is influenced by the stiffening mechanism since an active stiffening mechanism increases the stiffness of the endoscope thereby limiting its bending range and resulting in earlier saturation. The endoscope is unable is reach 0° due to this saturation and the involuntary activation of the jamming structure at higher pressures. This is clearly visible with the improved bending performance of the endoscope without the implementation of the jamming structure. The endoscope reaches a maximum bending angle of 40° and reaches upright position for an applied pressure of 0.21 bar. Variation in rest position between the two endoscopes is due to fabrication errors.

Hysteresis present is influenced by the movement of the jamming sheets contributing to the static friction of the module. Static friction is larger when the stiffening mechanism is active thereby increasing the hysteresis. However, for clinical applications, variable stiffness is only required for applying force and not during endoscopic motion.

Therefore, the advantage of the bent endoscope is that the non-linear start up transient has been reduced and shifted out of the center of the operating range. Finer control over the endoscope's angle near the straight configuration can be achieved by beginning in a bent position. Additionally, having only two pneumatic chambers enables downscaling of endoscope for surgical applications. Laminar jamming as a variable stiffening mechanism negatively influences the bending performance of the endoscope and further research is required for the implementation of variable stiffening mechanism.

IV. CONCLUSION

In conclusion, a novel pre-bent soft-surgical pneumatic endoscope with laminar jamming as the variable stiffening mechanism had been designed. It is shown that the bending performance of the endoscope, compared to similar work, has improved by both decreasing and shifting the start-up transient out of the operating range, thus, improving its controlability at small angles in the near-straight configuration. The variable stiffening mechanism, however, limits the bending range and its implementation needs to be further investigated.

REFERENCES

[1] T. N. Robinson and G. V. Stiegmann, "Minimally Invasive Surgery," *Endoscopy*, vol. 36, no. 1, pp. 48–51, jan 2004.

[2] S. A. Antoniou, G. A. Antoniou, A. I. Antoniou, and F. A. Granderath, "Past, present, and future of minimally invasive abdominal surgery," *Journal of the Society of Laparoendoscopic Surgeons*, vol. 19, no. 3, jul 2015. [Online]. Available: http://www.ncbi.nlm.nih.gov/pubmed/26508823http://www.pubmedcentral.nih.gov/articlerender.fcgi?artid=PMC4589904

[3] H. Abidi, G. Gerboni, M. Brancadoro, J. Fras, A. Diodato, M. Cianchetti, H. Wurdemann, K. Althoefer, and A. Menciassi, "Highly dexterous 2-module soft robot for intra-organ navigation in minimally invasive surgery," *International Journal of Medical Robotics and Computer Assisted Surgery*, vol. 14, no. 1, pp. 1–9, 2017.

[4] M. Runciman, A. Darzi, and G. P. Mylonas, "Soft Robotics in Minimally Invasive Surgery," *Soft Robotics*, vol. 6, no. 4, pp. 423–443, 2019.

[5] N. Kurniawan and M. Keuchel, "Flexible Gastro-intestinal Endoscopy — Clinical Challenges and Technical Achievements," pp. 168–179, jan 2017.

[6] S. Atallah, B. Martin-Perez, D. Keller, J. Burke, and L. Hunter, "Natural-orifice transluminal endoscopic surgery," *British Journal of Surgery*, vol. 102, no. 2, pp. 73–92, jan 2015. [Online]. Available: http://doi.wiley.com/10.1002/bjs.9710

[7] H. Xin, J. S. Zelek, and H. Carnahan, "Laparoscopic surgery, perceptual limitations and force: A review," *First Canadian Student Conference on Biomedical Computing*, no. January, pp. 44–46, 2006.

[8] Y. J. Kim, S. Cheng, S. Kim, and K. Iagnemma, "A novel layer jamming mechanism with tunable stiffness capability for minimally invasive surgery," *IEEE Transactions on Robotics*, vol. 29, no. 4, pp. 1031–1042, 2013.

[9] M. W. Gifari, H. Naghibi, S. Stramigioli, and M. Abayazid, "A review on recent advances in soft surgical robots for endoscopic applications," *International Journal of Medical Robotics and Computer Assisted Surgery*, vol. 15, no. 5, pp. 1–11, 2019.

[10] D. Rus and M. T. Tolley, "Design, fabrication and control of soft robots," *Nature*, vol. 521, no. 7553, pp. 467–475, 2015.

[11] P. Polygerinos, N. Correll, S. A. Morin, B. Mosadegh, C. D. Onal, K. Petersen, M. Cianchetti, M. T. Tolley, and R. F. Shepherd, "Soft Robotics: Review of Fluid-Driven Intrinsically Soft Devices; Manufacturing, Sensing, Control, and Applications in Human-Robot Interaction," *Advanced Engineering Materials*, vol. 19, no. 12, 2017.

[12] M. Cianchetti, T. Ranzani, G. Gerboni, I. De Falco, C. Laschi, and A. Menciassi, "STIFF-FLOP surgical manipulator: Mechanical design and experimental characterization of the single module," *IEEE International Conference on Intelligent Robots and Systems*, no. August, pp. 3576–3581, 2013.

[13] J. A. Lenssen, H. Naghibi, and M. Abayazid, "Evaluation of design aspects of modular pneumatic soft robotic endoscopes," in *2019 2nd IEEE International Conference on Soft Robotics (RoboSoft)*, 2019, pp. 56–61.

[14] M. Cianchetti and A. Menciassi, "Soft Robotics: Trends, Applications and Challenges," *Biosystems and Biorobotics*, vol. 17, pp. 75–85, 2017. [Online]. Available: http://link.springer.com/10.1007/978-3-319-46460-2

[15] L. Blanc, A. Delchambre, and P. Lambert, "Flexible medical devices: Review of controllable stiffness solutions," *Actuators*, vol. 6, no. 3, pp. 1–31, 2017.

[16] H. Naghibi, M. W. Gifari, W. Hoitzing, J. W. Lageveen, D. M. M. van As, S. Stramigioli, and M. Abayazid, "Development of a multi-level stiffness soft robotic module with force haptic feedback for endoscopic applications*," in *2019 International Conference on Robotics and Automation (ICRA)*, 2019, pp. 1527–1533.

[17] Y. Kim, S. S. Cheng, M. Diakite, R. P. Gullapalli, J. M. Simard, and J. P. Desai, "Toward the development of a flexible mesoscale MRI-compatible neurosurgical continuum robot," *IEEE Transactions on Robotics*, vol. 33, no. 6, pp. 1386–1397, dec 2017.

[18] B. S. Peters, P. R. Armijo, C. Krause, S. A. Choudhury, and D. Oleynikov, "Review of emerging surgical robotic technology," pp. 1636–1655, apr 2018.

[19] C. J. Kahi, P. Saxena, and M. A. Khashab, "New Platforms and Devices in Colonoscopy," *Colonoscopy and Polypectomy, An Issue of Gastroenterology Clinics*, vol. 42, no. 3, pp. 671–688, 2013.

[20] C. K. Yeung, J. L. Cheung, and B. Sreedhar, "Emerging next-generation robotic colonoscopy systems towards painless colonoscopy," *Journal of Digestive Diseases*, vol. 20, no. 4, pp. 196–205, apr 2019. [Online]. Available: https://onlinelibrary.wiley.com/doi/abs/10.1111/1751-2980.12718

[21] Olympus, "Extending the Art of Surgery to New Dimentions," pp. 1–3, 2019. [Online]. Available: https://medical.olympusamerica.com/products/endoeye

[22] B. P. M. Yeung and T. Gourlay, "A technical review of flexible endoscopic multitasking platforms," *International Journal of Surgery*, vol. 10, no. 7, pp. 345–354, 2012. [Online]. Available: http://dx.doi.org/10.1016/j.ijsu.2012.05.009

[23] Y. S. Narang, J. J. Vlassak, and R. D. Howe, "Mechanically Versatile Soft Machines through Laminar Jamming," *Advanced Functional Materials*, vol. 28, no. 17, p. 1707136, apr 2018. [Online]. Available: http://doi.wiley.com/10.1002/adfm.201707136

[24] G. Agarwal, N. Besuchet, B. Audergon, and J. Paik, "Stretchable Materials for Robust Soft Actuators towards Assistive Wearable Devices," *Scientific Reports*, vol. 6, no. 1, pp. 1–8, sep 2016. [Online]. Available: www.nature.com/scientificreports